



EPP-NO_x in Antarctic springtime stratospheric column: Evidence from observations and influence of the QBO

Emily Gordon¹, Annika Seppälä¹, and Johanna Tamminen²

¹Department of Physics, University of Otago, Dunedin, New Zealand

²Space and Earth Observation Centre, Finnish Meteorological Institute, Helsinki, Finland

Correspondence: Annika Seppälä (annika.seppala@otago.ac.nz)

Abstract. Observations from the Ozone Monitoring Instrument (OMI) on the Aura satellite are used to study the effect of energetic particle precipitation (EPP, as proxied by the geomagnetic activity index A_p) on the Antarctic stratospheric NO₂ column in late winter-spring (Aug-Dec) during the years 2005–2017. We show that the polar (60°S–90°S) stratospheric NO₂ column is significantly correlated with EPP throughout the Antarctic spring, until the breakdown of the polar vortex in November. The strongest correlation takes place during years with easterly phase of the quasi-biennial oscillation (QBO). We propose that the QBO affects the polar springtime EPP-NO_x in two ways: firstly by modulating the amount of the primary NO_x source, N₂O, transported to the polar region. Secondly, the QBO affects the temperature of the polar vortex and thus the amount of denitri-
5 fication occurring in the polar vortex, also verified from HNO₃ observations from the Microwave Limb Sounder (MLS/Aura). Our results suggest that NO_x produced by EPP significantly contributes to the stratospheric NO₂ column at the time when the
10 ozone hole is present in the Antarctic stratosphere. Based on our findings, we recommend that as chlorine activation continues to decrease in the Antarctic stratosphere, the total EPP-NO_x should be accounted for in predictions of Antarctic ozone recovery.

1 Introduction

In the polar stratosphere, the dominant source of odd nitrogen, NO_x (NO + NO₂), is produced via the oxidation of nitrous
15 oxide, N₂O (Brasseur and Solomon, 2005):



This reaction requires the presence of excited oxygen atoms O(¹D), which are produced in the atmosphere by photolysis of ozone (O₃) and thus depend on sunlight being present. As a result, NO production via reaction (1) only takes place outside polar winter conditions. Following reaction (1) the existing NO can be converted to NO₂ in reaction with ozone:





As N_2O production *in situ* in the polar stratosphere is insignificant, the polar stratospheric NO_x production is highly depen-
20 dant on the amount of N_2O transported from the tropics (Brasseur and Solomon, 2005). This principal source of polar N_2O is
injected from the troposphere into the stratosphere at equatorial latitudes. It is then transported towards the polar regions by
the large scale Brewer-Dobson circulation. The strength of the Brewer-Dobson circulation is modulated by the Quasi-Biennial
Oscillation (QBO): Strahan et al. (2015) have shown that the easterly/westerly phase of the QBO (at ~ 20 hPa) during the
Southern Hemisphere (SH) winter results in anomalously low/high Antarctic polar stratospheric N_2O in the following spring
25 (September).

The main pathway to NO_x loss is via photolysis (Brasseur and Solomon, 2005). During polar night conditions when little
to no sunlight is available, this results in long chemical lifetime (weeks to months) for the NO_x family. However, NO_x can
be removed from the lower stratosphere during the polar night in a process known as denitrification. This requires the winter
vortex to be cold enough that polar stratospheric clouds (PSCs) form. Denitrification occurs when reactive nitrogen (particularly
30 NO_2) is converted into HNO_3 in the lower stratosphere (Santee et al., 1995). HNO_3 is readily incorporated into PSCs, removing
gaseous HNO_3 from the lower stratosphere as it eventually falls into the troposphere via gravitational sedimentation (Brasseur
and Solomon, 2005).

It is now well established that precipitating energetic particles can drive large enhancements in NO_x quantities in the polar
atmosphere (see e.g. Seppälä et al., 2007; Funke et al., 2014a, b). Energetic particle precipitation (EPP) is the flux of charged
35 particles (protons and electrons) of solar and magnetospheric origin into the Earth's atmosphere. The charged particles are
guided to the polar regions by the Earth's magnetic field. Once reaching the atmosphere, they ionise the main neutral gases,
 N_2 and O_2 . The chain of ion-neutral reactions that follows the ionisation then leads to increases in NO_x species (this is known
as "EPP- NO_x "), particularly in the mesosphere and lower thermosphere (Brasseur and Solomon, 2005). EPP manifests as
energetic electron precipitation (EEP) as well as proton precipitation, which in the form of solar proton events (SPEs) is the
40 most extreme form of EPP (see e.g. Seppälä et al., 2014). SPEs are usually associated with coronal mass ejections (CMEs) and
thus, while the particles are highly energetic and have the ability to ionise as far down as the stratosphere, the events are short
(hours to days) in duration, and occur sporadically. Conversely, EEP is always present in some form and is mostly dependant on
solar wind speed (Funke et al., 2014b). Due to the lower energies of the electrons, EEP driven *in situ* NO_x increases typically
occur in the mesosphere and above (Turunen et al., 2009). When EPP occurs over the winter pole, the mesospheric NO_x has a
45 long chemical lifetime and can be transported downwards into the stratosphere inside the polar vortex. Once in the stratosphere,
these NO_x enhancements are effective at catalytically destroying ozone (see e.g., Jackman et al., 2008, and references therein).
As NO_x is not formed from N_2O during winter, EPP becomes a significant contributor to the polar winter NO_x budget (Funke
et al., 2014b).

Several previous studies have examined the effects of EPP on polar winter NO_x . We will summarise the findings of the key
50 observational works, with particular focus on those with SH or NO_x transport aspects, in the following.

Randall et al. (1998) reported stratospheric NO_2 observations from the Polar Ozone and Aerosol Measurement (POAM II)
over three polar late-winter/early-spring periods. They found evidence to suggest that NO_x from the SH polar mesosphere was
transported down into the stratosphere inside the polar vortex during the winter. They also suggested that the observed enhanced



55 levels of stratospheric NO_x in 1994 could be, at least partially, due to production by EPP that took place at higher altitudes before the downwards transport. Based on their analysis, Randall et al. (1998) suggested that NO_x transported to stratosphere from the mesosphere and above during the polar winter should be observable in Antarctic NO_2 column measurements.

Siskind et al. (2000) used Halogen Occultation Experiment (HALOE) observations from the UARS satellite between 1991-1996 to track NO_x enhancements in October in the SH polar region. They found that the year-to-year variability in NO_x inside the polar vortex followed variability in wintertime mean auroral A_p index, a measure now frequently used for overall EPP levels (Matthes et al., 2017). At the time, they found that the peak NO_x enhancements from "auroral" activity corresponded to around 3-5% of the total NO_x generated from N_2O . Studies of NO_x enhancements following the large Halloween SPEs in October-November 2003 also revealed large quantities of NO_x in the Northern Hemisphere (NH) in January (Jackman et al., 2005). However, dynamical effects, driven by the major sudden stratospheric warming (SSW) in December 2003, indicated that this NO_x was unlikely to have originated from the SPEs (Seppälä et al., 2007). The NO_x increases were more likely a result of the the large amounts of EEP that was present during the polar winter combined with downward descent. For example, Randall et al. (2005) used observations from a number of satellite instruments to show that the springtime NO_x increases in the NH were influenced by strong downward descent in January 2004, bringing excess amount of NO_x down to the stratosphere. Randall et al. (2007) used Atmospheric Chemistry Experiment-Fourier Transform Spectrometer (ACE-FTS) together with HALOE observations to show that the peak upper stratospheric EPP- NO_x was highly correlated with EEP levels over 1992-2005, up until September in the SH. Dynamics influencing the polar vortex is one of the main reason relations between NO_x observations and EPP break down. This is particularly important in the NH, where the polar vortex is more susceptible to SSWs. Randall et al. (2007) further found that the largest EPP- NO_x occurred during the declining phase of the solar cycle, during which more high-speed solar wind streams, driving EEP, are likely to occur.

Using tracer correlations to quantify EPP- NO_x vs NO_x from N_2O oxidation, Randall et al. (2007) suggested that the maximum EPP- NO_x enhancements made up to 40% of the total polar NO_y (total reactive nitrogen, $\text{NO}_y = \text{NO} + \text{NO}_2 + \text{NO}_3 + \text{ClONO}_2 + \text{HNO}_4 + \text{N}_2\text{O}_5 + \text{HNO}_3$) budget. Seppälä et al. (2007) contrasted average wintertime A_p levels with the polar winter upper-stratospheric-lower mesospheric NO_x observations from Global Ozone Monitoring by Occultation of Stars (GOMOS) onboard the Envisat satellite, finding a nearly linear relationship between the two during 2002-2006 for both hemispheres. Funke et al. (2014b) used Michelson Interferometer for Passive Atmospheric Sounding (MIPAS) observations, also from Envisat, of NO_y , to quantify the amount of EPP- NO_y in the polar winter. Analogous to Randall et al. (2007), they found that EPP- NO_y accounted for up to 40% of the wintertime polar NO_y . Funke et al. (2014a) then correlated A_p and EPP- NO_y in the wintertime and concluded that the strong relationship between A_p and EPP- NO_y supports using A_p as a proxy for tracking EPP- NO_y production in the SH wintertime.

Here, we use stratospheric NO_2 column observations from the Ozone Monitoring Instrument (OMI) on-board the Aura satellite to investigate EPP as a source of NO_x in the Antarctic later-winter - spring. Previous work suggested that EPP- NO_x makes up around 40% of the polar winter NO_x . We have a relatively long satellite period (2005-2017) in which to analyse how this NO_x propagates in the following springtime, and whether this detectable in the NO_2 column. We also analyse how the



phase of the QBO affects the contribution of EPP-NO₂ to the total NO₂ column in springtime, due to the modulation of the N₂O source.

90 2 Observations and Methods

2.1 OMI NO₂ observations

We use stratospheric NO₂ column observations from the Dutch-Finnish built Ozone Monitoring Instrument (OMI) on-board NASA's Aura satellite from August to December during years 2005–2017 (v3, Level 2 daily gridded NO₂, see Krotkov (2012); Krotkov et al. (2017)). The daily gridded data has 0.25° × 0.25° horizontal resolution. In our analysis, we use data from
95 latitudes poleward of 50°S. Aura is in a Sun-synchronous orbit, thus measurements take place at the same locations each year. While NO₂ notably has a diurnal cycle, using observations from the same sunlit locations (thus same local times) each year minimises the effect of this in our analysis.

The OMI-NO₂ data is provided as total column, as well as separated tropospheric and stratospheric columns. This separation is based on the location of the tropopause. Here, we use the OMI stratospheric column observations only. The effective vertical
100 range of the stratospheric column based on the OMI averaging kernels corresponds to ~ 15 – 35 km. The algorithm for the column separation is described in Bucseła et al. (2013). OMI measures back-scattered solar radiation from the atmosphere. Thus, observations are only available for solar illuminated locations – there is no coverage during polar night conditions. This horizontal coverage is illustrated in Figure 1, which presents the zonally averaged mean NO₂ column for the period under investigation (2005–2017). This shows how the NO₂ column varies in the polar springtime, with increasing amounts of NO₂
105 in the stratosphere as time progresses due to release from its reservoirs (Dirksen et al., 2011). The latitudinal coverage of the measurements is illustrated here, with the lack of measurements during the polar night leading to a gap at the highest latitudes during August-September. The error in the individual NO₂ column measurement is estimated to be < 2 × 10¹⁴ molecules cm⁻², however in areas with low levels of tropospheric pollution (such as the Southern polar region), this error is considerably less (Bucseła et al., 2013). Since June 2007, OMI-NO₂ has experienced an issue known as the row anomaly (RA) affecting certain
110 fields of view. All RA affected measurements have been excluded here, leaving around 2 × 10⁵ observations poleward of 60°S per day for the analysis period.

The Aug-Dec monthly mean polar (60°S to 90°S) average zonal mean NO₂ columns for each year are listed in Table 1.

2.2 MLS HNO₃ observations

We use HNO₃ profiles from NASA's Microwave Limb Sounder (MLS) which is also on-board the Aura satellite (Manney et al.,
115 2015). This study uses the version 4.2 product with data screened according to Livesey et al. (2017). MLS HNO₃ profiles have been validated by Santee et al. (2007). The latitude range used here is 60°S to around 82°S and the pressure range used is approximately 100 hPa to 10 hPa. This means using data from both the HNO₃ 240-GHz radiometer (for pressures ≥ 22 hPa) and HNO₃ 190-GHz radiometer (for pressures ≤ 15 hPa). MLS HNO₃ has vertical resolution of 3-4 km in the lower – middle

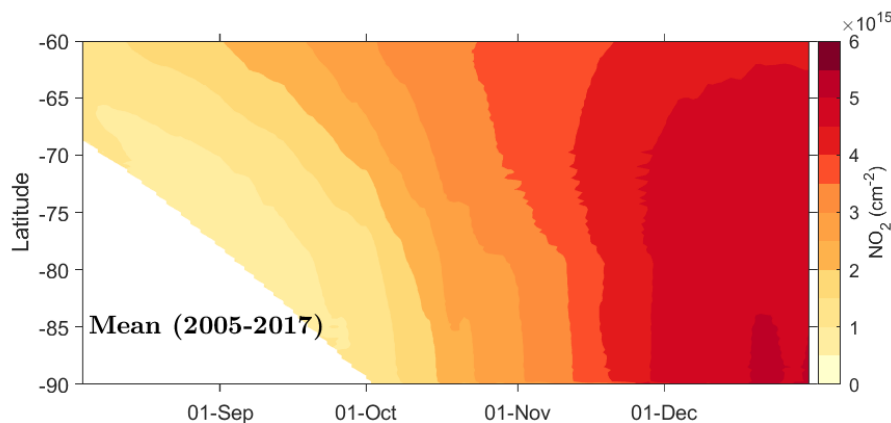


Figure 1. OMI 3 day running mean zonally averaged NO_2 column for the time period 2005–2017. The contour interval is $0.5 \times 10^{15} \text{ cm}^{-2}$. The white area at high latitudes in August-September indicates polar night conditions where OMI observations are not available.

stratosphere (used here) and the precision of individual profiles is around 0.6 ppbv in this region. The estimated error in these
120 profiles is no more than 10%.

2.3 EPP proxy

The geomagnetic activity index A_p is a well-established proxy for EPP (see e.g. Matthes et al., 2017; Funke et al., 2014b) and is used here to estimate the overall levels of EPP for each polar winter under investigation. During 2005–2017, the mean A_p was 8.5, reflecting the relatively low overall solar activity during solar cycle 24 (solar cycle 23 average was 12.9). To estimate
125 the overall EPP activity during each winter, we calculate the mean A_p for the period of May–August of each year. These means are hereafter referred to as \hat{A}_p and are provided in Table 1. We designate high \hat{A}_p (H- \hat{A}_p) winters as those with $\hat{A}_p > 8.5$, i.e. \hat{A}_p higher than the average for 2005–2017. Similarly, we take low \hat{A}_p winters (L- \hat{A}_p) as those with $\hat{A}_p < 8.5$. The variation in winter \hat{A}_p throughout this study is shown in Figure 2. This figure captures the 11-year solar cycle fairly well, with minimum around 2009 and maximum around 2015.

130 All correlations between the NO_2 columns and \hat{A}_p are based on the Spearman rank correlation (Spearman ρ), as it more robustly accounts for any non-linear relationships (Wilks, 2011) while still interpreting linear trends where present. Statistical significance is here defined as correlations significant at $\geq 95\%$.

2.4 Quasi Biennial Oscillation

To investigate the potential QBO effect in the Antarctic atmosphere, we estimate the phase of the QBO from the 25 hPa level
135 zonal mean zonal wind (Naujokat, 1986) near the equator in May each year (Strahan et al., 2015). For use of the 25 hPa level in the Southern Hemisphere, see Baldwin and Dunkerton (1998). We take months where the wind direction is easterly as easterly QBO (eQBO), and westerly as westerly QBO (wQBO). The QBO direction for each year of the study is indicated in

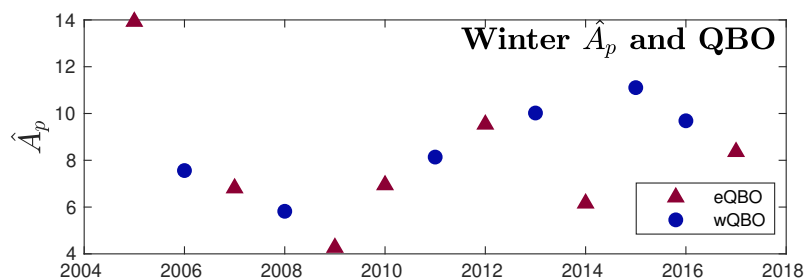


Figure 2. Mean wintertime A_p (\hat{A}_p) for each year of this study. The direction of the QBO at 25 hPa in May is indicated with red triangles representing eQBO and blue circles wQBO.

Table 1. May-Aug mean A_p (\hat{A}_p), the polar (60°S to 90°S) Aug-Dec monthly mean, zonal mean stratospheric NO_2 column density ($\times 10^{15} \text{ cm}^{-2}$), and QBO phase (E for easterly, W for westerly) for each year 2005-2017.

| Year | \hat{A}_p | Aug NO_2 | Sep NO_2 | Oct NO_2 | Nov NO_2 | Dec NO_2 | QBO |
|------|-------------|-------------------|-------------------|-------------------|-------------------|-------------------|-----|
| 2005 | 13.9 | 1.12 | 1.67 | 3.09 | 4.71 | 5.08 | E |
| 2006 | 7.6 | 0.96 | 1.22 | 2.36 | 3.54 | 5.01 | W |
| 2007 | 6.8 | 1.09 | 1.56 | 3.00 | 3.80 | 4.77 | E |
| 2008 | 5.8 | 0.95 | 1.22 | 2.71 | 3.79 | 4.92 | W |
| 2009 | 4.3 | 1.08 | 1.31 | 2.75 | 3.81 | 5.11 | E |
| 2010 | 6.9 | 1.13 | 1.50 | 2.76 | 3.80 | 4.60 | E |
| 2011 | 8.1 | 0.98 | 1.25 | 2.24 | 3.78 | 4.81 | W |
| 2012 | 9.5 | 1.23 | 1.67 | 3.51 | 4.45 | 4.83 | E |
| 2013 | 10.0 | 1.04 | 1.56 | 3.23 | 4.74 | 5.04 | W |
| 2014 | 6.2 | 1.03 | 1.40 | 2.71 | 4.17 | 4.96 | E |
| 2015 | 11.1 | 0.94 | 1.34 | 2.15 | 3.69 | 4.62 | W |
| 2016 | 9.7 | 1.10 | 1.45 | 2.74 | 4.39 | 4.79 | W |
| 2017 | 8.4 | 1.08 | 1.56 | 2.72 | 4.51 | 4.88 | E |

both Table 1 and Figure 2. Figure 2 illustrates the approximately biennial nature of the oscillation, with the direction changing almost every year.

140 3 Results

3.1 NO_2 anomalies

Figure 3 presents the average anomaly, i.e. the mean deducted for each of the four different categories of this study, eQBO H- \hat{A}_p , eQBO L- \hat{A}_p , wQBO H- \hat{A}_p , and wQBO L- \hat{A}_p . We can see that winter \hat{A}_p affects the column NO_2 present in the spring:

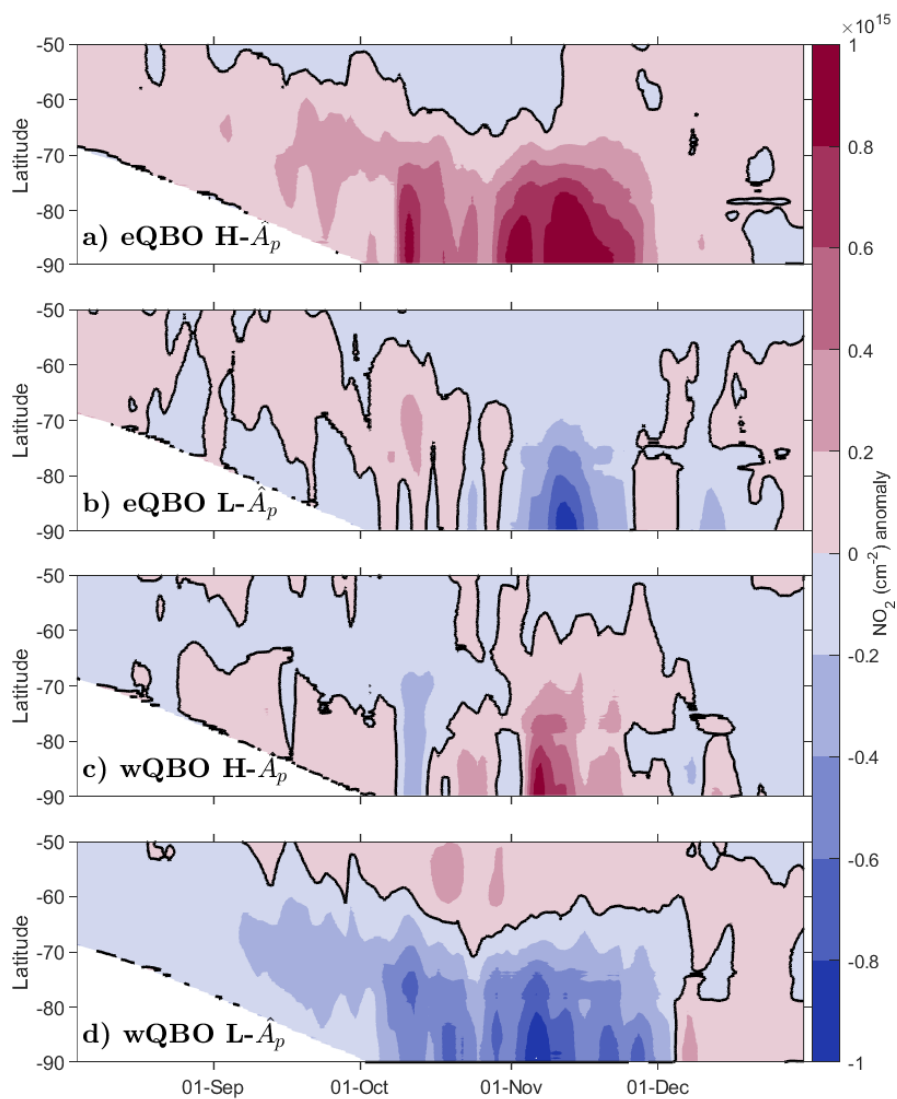


Figure 3. a) mean NO₂ anomaly for years with both H- \hat{A}_p and eQBO. Contour level is $0.2 \times 10^{15} \text{ cm}^{-2}$ with black contour representing zero anomaly. b)-d) as b) but different combinations of \hat{A}_p and QBO (see Figure).

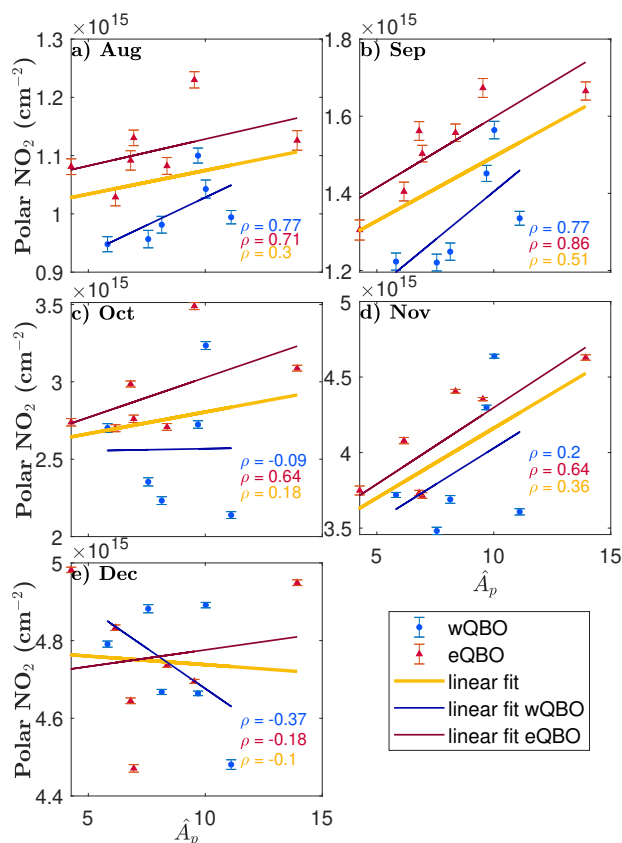


Figure 4. \hat{A}_p versus monthly average NO₂ column density averaged over 60°S to 90°S (where available, see text) for the months of August to December (months as shown in each individual panel). Red triangles indicate years with eQBO and blue circles years with wQBO. Yellow line shows a linear fit to all data, red line eQBO years only, and blue line wQBO years only. The Spearman ρ (correlation coefficient) for each set is shown in each with corresponding colour, e.g. red ρ corresponds to correlation coefficient for eQBO years etc.. Error bars are 2 × the standard error in the mean.

years with H- \hat{A}_p (panels a and c) having more positive anomalies from August to November especially in the highest latitudes. In b) and c), the month of October is highly variable with both showing regions of positive and negative anomaly. For low \hat{A}_p years (panels b and d) early spring is not consistently positive or negative, however November displays negative anomalies at high latitudes. The QBO influence appears to be most significant for H- \hat{A}_p eQBO years, and wQBO L- \hat{A}_p years (panels a and d). These show consistent but opposite behaviour throughout the spring, with H- \hat{A}_p eQBO years the most favourable for NO₂ and wQBO L- \hat{A}_p the least.

150 3.2 Mean SH polar columns

Figure 4 presents the \hat{A}_p and the mean polar (60°S–90°S) NO₂ column for each year (2005–2017) and for each individual month from August to December. The phase of the QBO in the preceding May is indicated with red triangles corresponding



to eQBO and blue circles to wQBO conditions. Linear fits for all years, wQBO, and eQBO years are included in each panel to guide the eye. The Spearman correlation coefficient (ρ) for each month for all years (yellow) along with eQBO (red) and
155 wQBO (blue) years only are also included in the panels. Note that, as the OMI measurement field gradually increases from an initial maximum latitude of around 68°S in August to 90°S by the end of September, the total NO_2 column values do not initially fully encompass the entire polar region (60°S – 90°S).

The results shown in Figure 4 suggests that a correlation between \hat{A}_p and the stratospheric NO_2 column occurs in August, September and November. This is consistent with Figure 3. Furthermore, there is a clear positive correlation for eQBO years
160 from August to November, while for wQBO years, the positive correlation in August and September disappears in October. While the wQBO November linear fit is close to the total fit, the individual years show large variability. In general, wQBO years have consistently lower column NO_2 values, especially in August and September.

To contrast our results with previous extensive work by Funke et al. (2014a) we repeated the analysis presented in Figure 4 using the units of gigamole (Gmol, see Funke et al. (2016)) for the monthly mean polar NO_2 columns. This figure is included
165 in the appendix as Figure A1 and shows the least squares linear fits, with the corresponding parameters given in each panel. This allows us to estimate the linear EPP- NO_x contribution to the lower stratosphere (~ 15 – 35 km) in the spring, analogous to Funke et al. (2014a). For example, in September (Figure A1, panel b), the approximate contribution to polar stratospheric NO_2 column from EPP in eQBO years is $+0.021$ Gmol/ \hat{A}_p . The largest contribution to lower stratospheric NO_2 from EPP occurs in November for both eQBO and wQBO years as well as all years in general, with the corresponding values of $+0.058$, $+0.055$
170 and $+0.052$ Gmol/ \hat{A}_p , respectively. Funke et al. (2014a) (see their Figure 10, showing excess EPP- NO_y in the stratosphere – lower mesosphere in early spring) found an increase in SH polar EPP- NO_y of around $+0.0698$ Gmol/ A_p unit in September. Contrasting this to our results of up to $+0.058$ Gmol/ \hat{A}_p in November, it seems a large fraction of the EPP- NO_y detected by Funke et al. (2014a) is maintained in the polar region and able to reach the lower stratosphere by November. Note that Funke et al. (2014a) use a weighted A_p scheme.

175 3.3 Latitudinal correlations

Figure 5 shows the latitudinal extent of the correlation between \hat{A}_p and the 7 day running mean NO_2 column for latitudes 50°S – 90°S averaged over 1° latitude bins. Panel a) presents the correlation when all years are taken into account. Significant positive correlation occurs in late August and variably throughout September, then again in November. October and December show little to no significant correlation. Panel b) shows the correlation for eQBO years only. There are areas of statistically
180 significant positive correlations in all months except December. In October, significant correlations occur only at the very beginning of the month. High positive correlations are still present across 60°S to 90°S from early to mid-November providing first evidence of the indirect EPP- NO_x effect lasting well into the SH spring season. Figure 5 c) presents correlation for years with wQBO only. While positive correlations are present throughout August and September, only small regions are found to be statistically significant. October marks a shift towards negative correlation (not statistically significant) at all latitudes. In
185 November the correlations turn positive once more, but these are again, not statistically significant.

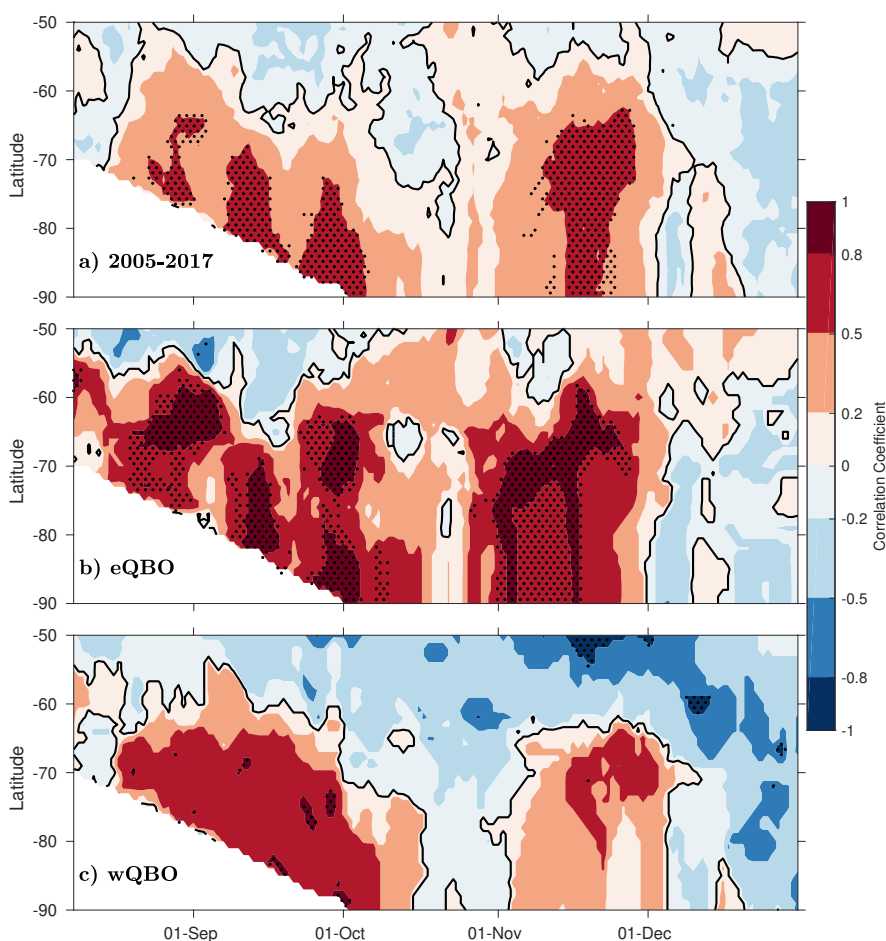


Figure 5. a) Correlation of \hat{A}_p and 7 day running mean NO_2 column density for Aug-Dec for all years. b) Correlation of \hat{A}_p and 7 day running mean NO_2 column density for years with eQBO only. c) as b) except for years with wQBO only. All figures have 1° latitude resolution. Contour levels are shown for [-1, -0.8, -0.5, -0.2, 0, 0.2, 0.5, 0.8, 1] and the zero contour is indicated with black. Stippling shows regions of correlation significant at $\geq 95\%$ level.



The results from Figure 5 suggest that the NO_2 column increases at high polar latitudes in September are due to higher than average EPP/geomagnetic activity, as strong correlations between NO_2 and \hat{A}_p occur in all panels. They also imply that increases in NO_2 in November can be due to a combination of high EPP activity and eQBO, whereas wQBO appears to reduce the significance of any EPP induced NO_2 increases.

190 4 Discussion

4.1 Polar vortex influence in October

The correlations presented in previous sections were found to be less significant in October, only to increase again in November. As this time of year marks the typical breakup period of the polar vortex (Hurwitz et al., 2010) and knowing that the descent of EPP produced NO_x is limited to inside the polar vortex (as previously demonstrated for October by Siskind et al. (2000)),
195 we will now investigate the month of October separately, taking the polar vortex into account.

To account for effects from potential asymmetries in the shape of the polar vortex in October in our zonal mean calculations, we repeated the earlier analysis for measurements located inside the vortex. To establish the location of the edge of the polar vortex we utilised the OMI co-located ozone column measurements (Bhartia, 2012): Ozone depleted air is isolated within the vortex until the vortex break up, typically in late November (Kuttippurath and Nair, 2017). Based on this, we take measurement
200 locations poleward of 50°S with corresponding stratospheric ozone column of < 245 DU to be inside the polar vortex. An example of how the ozone column and the estimated vortex edge are reflected on the NO_2 column measurement is shown in Figure 6.

Figure 7 shows the October results (as in Figures 4 c and 5 b) when only observations inside the polar vortex are included. We find that for eQBO, the observations are now much closer to the linear fit than in Figure 4 c), implying that the earlier
205 disappearance of correlation was likely due to variations in the shape of the polar vortex in October.

Similarly for the horizontal distribution of the correlations, we now find strong correlations for eQBO years throughout October. This again implies that the lack of correlation in October is due to the distorted shape of the polar vortex being smeared out by calculation of zonal means, and the effect of EPP on the NO_2 column is significant through October. The reappearance of correlations in eQBO years in November is likely a mixing effect, with the break down of the polar vortex
210 around this time leading to vortex air being mixed with extra-vortex air, and thus the net effect on the NO_2 column is still observable.

Although the A_p index is generally much lower now than in the 1991-1996 period investigated by Siskind et al. (2000), considering observations only in the vortex still shows the same, strong linear relationship found in that study. This implies that solar activity of any level generates a proportional response in reactive nitrogen.

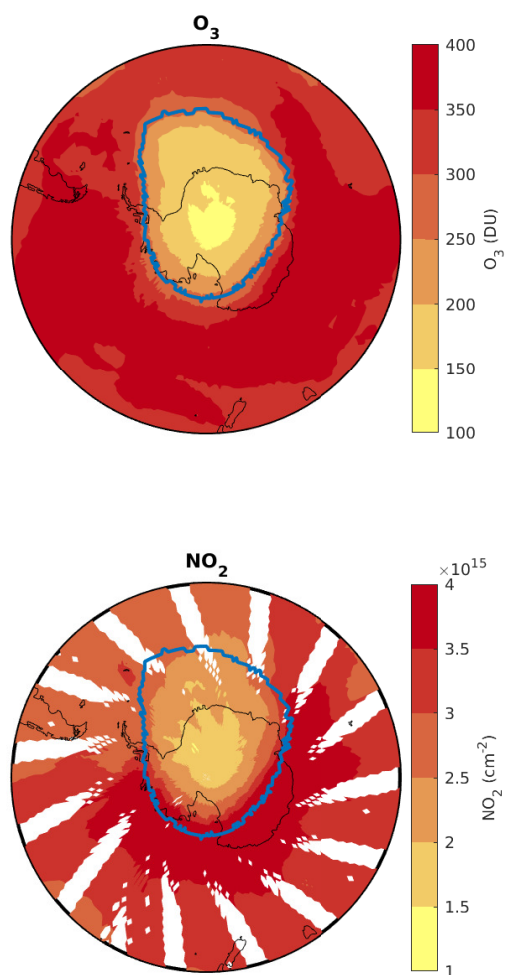


Figure 6. Vortex edge identification based on OMI ozone column. The top panel shows the OMI measured ozone column density with the 245 DU contour highlighted. The bottom panel shows the NO_2 stratospheric column with the 245 DU ozone contour overlaid.

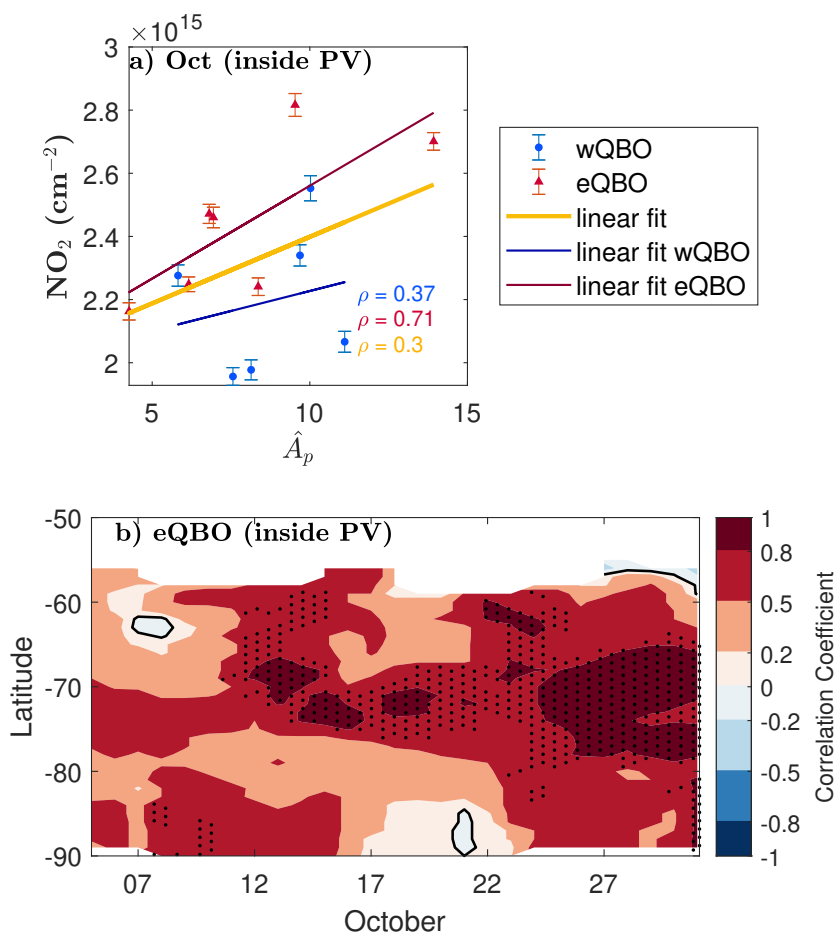


Figure 7. a) \hat{A}_p vs. the average NO₂ from 60°S to 90°S, for observations inside the polar vortex. Red triangles correspond to eQBO years and blue circles to wQBO years. The yellow line represents a linear fit to all data points, while the red line is for eQBO years only and blue for wQBO years only. ρ values are as in Figure 4. Error bars indicate the 95% confidence interval for the mean. b) Correlation of \hat{A}_p with 5 day running mean NO₂ column inside the polar vortex for eQBO years. Contour levels are shown for [-1, -0.8, -0.5, -0.2, 0, 0.2, 0.5, 0.8, 1], with an additional black line for the zero contour. The stippling indicates correlations significant at $\geq 95\%$ level.

215 4.2 Influence of the QBO

As shown in Figures 3, 4 and 5 a), our results suggest the that phase of the QBO is influencing the SH polar EPP-NO_x signal in the spring months. Strahan et al. (2015) found that eQBO phase in early winter leads to decreased N₂O in the high polar stratosphere in September. Figure 1 of Strahan et al. (2015) clearly shows a negative anomaly for N₂O in September in eQBO

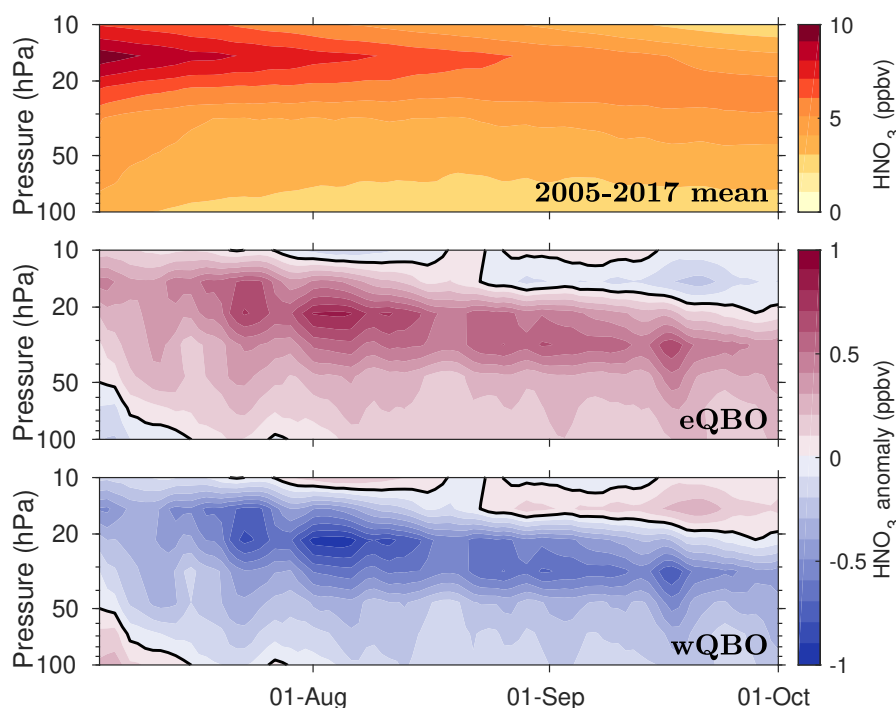


Figure 8. a) 3 day running mean HNO_3 volume mixing ratio from 60°S to 82°S for the lower stratosphere for 2005-2017 late winter–early spring. Contour interval is 1 ppbv. b) HNO_3 anomaly from the mean for years with eQBO. Contour interval is 0.1 ppbv, with black contour showing zero anomaly. c) as b) but for wQBO years.

years for the upper Antarctic stratosphere. Our results suggest that the lack of N_2O transported to the polar regions during
220 eQBO years means that EPP- NO_x contributes more to the overall SH polar stratospheric NO_x in the springtime.

4.3 PSCs and denitrification

The affected transport of N_2O does not however explain the obviously depleted in NO_2 in wQBO years in Figure 4). This is
225 due to a different effect of the QBO on the polar region. Baldwin and Dunkerton (1998) found that the polar vortex is colder during winters with wQBO. Colder polar vortex results in a higher likelihood of polar stratospheric cloud (PSC) formation
(Brasseur and Solomon, 2005). As discussed earlier, PSCs affect the heterogeneous chemistry in the polar region, leading to
denitrification of the lower stratosphere (Dirksen et al., 2011). So for years with more PSCs (i.e. wQBO) we would expect more
denitrification to occur, resulting in the depleted NO_2 column reported here, also explaining the lower incidence of significant
correlation for these years.



To test whether QBO direction affects denitrification in the Antarctic stratosphere, we use HNO_3 observations from MLS
230 (see section 2.2). Figure 8 a) shows the mean HNO_3 from 60°S to 82°S for 2005-2017 over the late winter–early spring period,
i.e. when the polar vortex is coldest and PSCs are forming. Panels b) and c) show the anomalies from the mean for eQBO and
wQBO years respectively. The vertical pressure range of all three panels is 100 hPa to 10 hPa which corresponds to an altitude
range of approximately 17 km to 32 km. As can be seen in Figure 8, eQBO years tend to have more HNO_3 (up to 1 ppbv)
throughout this period, while wQBO years show a consistently negative anomaly (up to -1 ppbv). This clearly implies that
235 more HNO_3 is being removed from the stratosphere in wQBO years than in eQBO years. This supports our hypothesis that
wQBO causes more denitrification and thus depletes NO_x , contributing to the results in Figures 3–5.

5 Conclusions

We have, for the first time, traced EPP- NO_2 in the Antarctic stratospheric column in the late springtime using OMI/Aura
stratospheric NO_2 column observations. This is one of the few studies to use stratospheric NO_2 data from OMI and also
240 highlights the value of long time series of stratospheric NO_2 from nadir viewing instruments. Our analysis shows that influence
from the QBO is able to mask the stratospheric EPP- NO_x signal in satellite observations in a way that to our knowledge has
not previously been accounted for: Increased EPP during the winter, when combined with eQBO phase, results in enhanced
EPP- NO_x in the polar stratospheric column until late November.

The QBO influence is likely due to a combination of two effects: 1) eQBO reduces transport of N_2O to the polar region
245 (Strahan et al., 2015) resulting in a reduced background NO_x source in eQBO years. Thus enhancements in EPP- NO_x become
more evident in the springtime; 2) eQBO conditions reduce the probability of PSC formation, and as a result EPP- NO_x is
less likely to be removed by denitrification during the winter/early spring. This is also supported by MLS HNO_3 observations,
showing less denitrification during eQBO years.

Previously, Funke et al. (2014a) analysed EPP- NO_y observations and were able to attribute SH enhancements of $+0.0698 \text{ Gmol}/\text{A}_p$
250 into early spring months (September). Here, we show that this reactive nitrogen lingers, entering the lower stratosphere in the
form of NO_2 at an average rate of $+0.052 \text{ Gmol}/\hat{\text{A}}_p$ in November.

We present evidence of contribution from EPP- NO_x in the Antarctic stratosphere at a time when the ozone hole is present.
 NO_x is well known to react with both ozone and active halogens, catalytically destroying the former, and driving the latter to its
reservoirs (Brasseur and Solomon, 2005). Antarctic ozone loss has been found to be reduced in years with eQBO (Garcia and
255 Solomon, 1987) due (at least in part) to the increased vortex temperatures hampering chlorine activation on PSCs (Lait et al.,
1989). Our results suggest that as chlorine activation continues to decrease in the Antarctic stratosphere following the Montreal
Protocol (Solomon et al., 2016), the total EPP- NO_x (in addition to SPEs as pointed out by Stone et al., 2018) in eQBO years
needs to be accounted for in predictions of Antarctic springtime ozone recovery. Future studies should investigate the effects
of EPP- NO_x on the fragile ozone chemistry in the springtime and how this is modulated by the QBO.

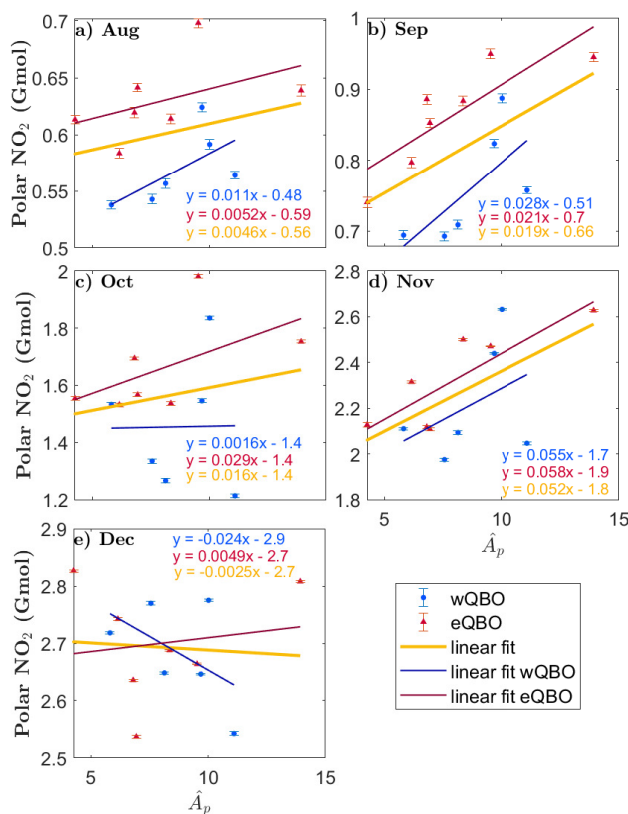


Figure A1. As Figure 4, but with monthly average polar NO_2 expressed in gigamole (Gmol). Each panel shows the linear least squares fit to data points (colour coding as before), including the fit equations ($y = \text{NO}_2$, $x = \hat{A}_p$). Red triangles are years with eQBO, and blue circles are wQBO. The yellow linear fit is a best-fit line for all the data in each plot, while the red fits only eQBO data, and the blue line fits only wQBO data.

260 **Data availability.** All data used here are open access and available from the following sources: A_p : <http://wdc.kugi.kyoto-u.ac.jp/kp/>; QBO: <https://www.geo.fu-berlin.de/en/met/ag/strat/produkte/qbo/>; OMI and MLS: <https://earthdata.nasa.gov/>.

Author contributions. EMG and AS planned the study. EMG did the analysis with support from AS. JT provided expertise on OMI observations. EMG and AS lead the writing of the manuscript with comments from all authors.

Competing interests. The authors declare no competing interests.



265 *Acknowledgements.* We are grateful for the World Data Center for Geomagnetism, the Freie Universität Berlin and the National Aeronautics and Space Administration for providing open access to the data sets used in this study. We would like to thank Dan Smale and Cora Randall for their useful discussions and valuable feedback.



References

- Baldwin, M. P. and Dunkerton, T. J.: Quasi-biennial modulation of the southern hemisphere stratospheric polar vortex, *Geophys. Res. Lett.*, 25, 3343–3346, <https://doi.org/10.1029/98GL02445>, 1998.
- Bhartia, P. K.: OMI/Aura Ozone (O₃) Total Column Daily L2 Global Gridded 0.25 degree × 0.25 degree V3, <https://doi.org/10.5067/Aura/OMI/DATA2025>, Accessed: [12/11/2018], 2012.
- Brasseur, G. P. and Solomon, S.: *Aeronomy of the Middle Atmosphere*, Springer, 2005.
- Bucsela, E. J., Krotkov, N. A., Celarier, E. A., Lamsal, L. N., Swartz, W. H., Bhartia, P. K., Boersma, K. F., Veeffkind, J. P., Gleason, J. F., and Pickering, K. E.: A new stratospheric and tropospheric NO₂ retrieval algorithm for nadir-viewing satellite instruments: applications to OMI, *Atmos. Meas. Tech.*, 6, 2607–2626, <https://doi.org/10.5194/amt-6-2607-2013>, 2013.
- Dirksen, R. J., Boersma, K. F., Eskes, H. J., Ionov, D. V., Bucsela, E. J., Levelt, P. F., and Kelder, H. M.: Evaluation of stratospheric NO₂ retrieved from the Ozone Monitoring Instrument: Intercomparison, diurnal cycle, and trending, *J. Geophys. Res.: Atmos.*, 116, D08 305, <https://doi.org/10.1029/2010JD014943>, 2011.
- Funke, B., López-Puertas, M., Holt, L., Randall, C. E., Stiller, G. P., and von Clarmann, T.: Hemispheric distributions and interannual variability of NO_y produced by energetic particle precipitation in 2002–2012, *J. Geophys. Res.: Atmos.*, 119, 13,565–13,582, <https://doi.org/10.1002/2014JD022423>, 2014a.
- Funke, B., López-Puertas, M., Stiller, G. P., and von Clarmann, T.: Mesospheric and stratospheric NO_y produced by energetic particle precipitation during 2002–2012, *J. Geophys. Res.: Atmos.*, 119, 4429–4446, <https://doi.org/10.1002/2013JD021404>, 2014b.
- Funke, B., López-Puertas, M., Stiller, G., Versick, S., and Clarmann, T.: A semi-empirical model for mesospheric and stratospheric NO_y produced by energetic particle precipitation, *Atmos. Chem. Phys.*, 16, 8667–8693, <https://doi.org/10.5194/acp-16-8667-2016>, 2016.
- Garcia, R. R. and Solomon, S.: A possible relationship between interannual variability in Antarctic ozone and the quasi-biennial oscillation, *Geophys. Res. Lett.*, 14, 848–851, <https://doi.org/10.1029/GL014i008p00848>, 1987.
- Hurwitz, M. M., Newman, P. A., Li, F., Oman, L. D., Morgenstern, O., Braesicke, P., and Pyle, J. A.: Assessment of the breakup of the Antarctic polar vortex in two new chemistry-climate models, *J. Geophys. Res.: Atmos.*, 115, <https://doi.org/10.1029/2009JD012788>, 2010.
- Jackman, C. H., DeLand, M. T., Labow, G. J., Fleming, E. L., Weisenstein, D. K., Ko, M. K. W., Sinnhuber, M., and Russell, J. M.: Neutral atmospheric influences of the solar proton events in October–November 2003, *J. Geophys. Res.: Space Phys.*, 110, A09S27, <https://doi.org/10.1029/2004JA010888>, 2005.
- Jackman, C. H., Marsh, D. R., Vitt, F. M., Garcia, R. R., Fleming, E. L., Labow, G. J., Randall, C. E., López-Puertas, M., Funke, B., von Clarmann, T., and Stiller, G. P.: Short- and medium-term atmospheric constituent effects of very large solar proton events, *Atmos. Chem. Phys.*, 8, 765–785, <https://doi.org/10.5194/acp-8-765-2008>, 2008.
- Krotkov, N. A.: OMI/Aura NO₂ Total and Tropospheric Column Daily L2 Global Gridded 0.25 degree × 0.25 degree V3, <https://doi.org/10.5067/Aura/OMI/DATA2018>, Accessed: [12/11/2018], 2012.
- Krotkov, N. A., Lamsal, L. N., Celarier, E. A., Swartz, W. H., Marchenko, S. V., Bucsela, E. J., Chan, K. L., Wenig, M., and Zara, M.: The version 3 OMI NO₂ standard product, *Atmos. Meas. Tech.*, 10, 3133–3149, <https://doi.org/10.5194/amt-10-3133-2017>, 2017.
- Kuttippurath, J. and Nair, P.: The signs of Antarctic ozone hole recovery, *Scientific Reports*, 7, 585, <https://doi.org/10.1038/s41598-017-00722-7>, 2017.



- Lait, L. R., Schoeberl, M. R., and Newman, P. A.: Quasi-biennial modulation of the Antarctic ozone depletion, *J. Geophys. Res.: Atmos.*, 94, 11 559–11 571, <https://doi.org/10.1029/JD094iD09p11559>, 1989.
- Livesey, N. J., Read, W. G., Wagner, P. A., Froidevaux, L., Lambert, A., Manney, G. L., Millán Valle, L. F., Hugh C. Pumphrey, H. C., Santee, M. L., Schwartz, M. J., Wang, S., Fuller, R. A., Jarnot, R. F., Knosp, B. W., Martinez, E., and Lay, R. R.: Earth Observing System (EOS) Aura Microwave Limb Sounder (MLS) version 4.2x level 2 data quality and description document, https://mls.jpl.nasa.gov/data/v4-2_data_quality_document.pdf, 2017.
- 310 Manney, G., Santee, M., Froidevaux, L., Livesey, N., and Read, W.: MLS/Aura Level 2 Nitric Acid (HNO₃) Mixing Ratio V004, <https://doi.org/10.5067/Aura/MLS/DATA2012>, Accessed: [29/08/2019], 2015.
- Matthes, K., Funke, B., Andersson, M. E., Barnard, L., Beer, J., Charbonneau, P., Clilverd, M. A., Dudok de Wit, T., Haberreiter, M., Hendry, A., Jackman, C. H., Kretzschmar, M., Kruschke, T., Kunze, M., Langematz, U., Marsh, D. R., Maycock, A. C., Misios, S., Rodger, C. J., Scaife, A., Seppälä, A., Shangguan, M., Sinnhuber, M., Tourpali, K., Usoskin, I., Van De Kamp, M., Verronen, P. T., and Versick, S.: Solar forcing for CMIP6 (v3.2), *Geosci. Model Dev.*, 10, 2247–2302, <https://doi.org/10.5194/gmd-10-2247-2017>, 2017.
- 315 Naujokat, B.: An Update of the Observed Quasi-Biennial Oscillation of the Stratospheric Winds over the Tropics, *J. Atmos. Sci.*, 43, 1873–1877, [https://doi.org/10.1175/1520-0469\(1986\)043<1873:AUOTOQ>2.0.CO;2](https://doi.org/10.1175/1520-0469(1986)043<1873:AUOTOQ>2.0.CO;2), 1986.
- Randall, C. E., Rusch, D. W., Bevilacqua, R. M., Hoppel, K. W., and Lumpe, J. D.: Polar Ozone and Aerosol Measurement (POAM) II stratospheric NO₂, 1993–1996, *J. Geophys. Res.: Atmos.*, 103, 28,361–28,371, <https://doi.org/10.1029/98JD02092>, 1998.
- 320 Randall, C. E., Harvey, V. L., Manney, G. L., Orsolini, Y., Codrescu, M., Sioris, C., Brohede, S., Haley, C. S., Gordley, L. L., Zawodny, J. M., and Russell, J. M.: Stratospheric effects of energetic particle precipitation in 2003–2004, *Geophys. Res. Lett.*, 32, L05 802, <https://doi.org/10.1029/2004GL022003>, 2005.
- Randall, C. E., Harvey, V. L., Singleton, C. S., Bailey, S. M., Bernath, P. F., Codrescu, M., Nakajima, H., and Russell, J. M.: Energetic particle precipitation effects on the Southern Hemisphere stratosphere in 1992–2005, *J. Geophys. Res.*, 112, D08 308, <https://doi.org/10.1029/2006JD007696>, 2007.
- 325 Santee, M. L., Read, W. G., Waters, J. W., Froidevaux, L., Manney, G. L., Flower, D. A., Jarnot, R. F., Harwood, R. S., and Peckham, G. E.: Interhemispheric Differences in Polar Stratospheric HNO₃, H₂O, ClO, and O₃, *Science*, 267, 849–852, <https://doi.org/10.1126/science.267.5199.849>, 1995.
- Santee, M. L., Lambert, A., Read, W. G., Livesey, N. J., Cofield, R. E., Cuddy, D. T., Daffer, W. H., Drouin, B. J., Froidevaux, L., Fuller, R. A., Jarnot, R. F., Knosp, B. W., Manney, G. L., Perun, V. S., Snyder, W. V., Stek, P. C., Thurstans, R. P., Wagner, P. A., Waters, J. W., Muscari, G., de Zafra, R. L., Dibb, J. E., Fahey, D. W., Popp, P. J., Marcy, T. P., Jucks, K. W., Toon, G. C., Stachnik, R. A., Bernath, P. F., Boone, C. D., Walker, K. A., Urban, J., and Murtagh, D.: Validation of the Aura Microwave Limb Sounder HNO₃ measurements, *J. Geophys. Res.: Atmos.*, 112, <https://doi.org/10.1029/2007JD008721>, 2007.
- 330 Seppälä, A., Clilverd, M. A., and Rodger, C. J.: NO_x enhancements in the middle atmosphere during 2003–2004 polar winter: Relative significance of solar proton events and the aurora as a source, *J. Geophys. Res.*, 112, D23 303, <https://doi.org/10.1029/2006JD008326>, 2007.
- 335 Seppälä, A., Verronen, P. T., Clilverd, M. A., Randall, C. E., Tamminen, J., Sofieva, V., Backman, L., and Kyölä, E.: Arctic and Antarctic polar winter NO_x and energetic particle precipitation in 2002–2006, *Geophys. Res. Lett.*, 34, L12 810, <https://doi.org/10.1029/2007GL029733>, 2007.
- 340 Seppälä, A., Matthes, K., Randall, C. E., and Mironova, I. A.: What is the solar influence on climate? Overview of activities during CAWSES-II, *Prog. Earth Planet. Sci.*, 1, 24, <https://doi.org/10.1186/s40645-014-0024-3>, 2014.



- Siskind, D. E., Nedoluha, G. E., Randall, C. E., Fromm, M., and Russell III, J. M.: An assessment of Southern Hemisphere stratospheric NO_x enhancements due to transport from the upper atmosphere, *Geophys. Res. Lett.*, 27, 329–332, <https://doi.org/10.1029/1999GL010940>, 2000.
- 345 Solomon, S., Ivy, D. J., Kinnison, D. E., Mills, M. J., Neely, R. R., and Schmidt, A.: Emergence of healing in the Antarctic ozone layer, *Science*, <https://doi.org/10.1126/science.aae0061>, 2016.
- Stone, K. A., Solomon, S., and Kinnison, D. E.: On the Identification of Ozone Recovery, *Geophys. Res. Lett.*, 45, 5158–5165, <https://doi.org/10.1029/2018GL077955>, 2018.
- Strahan, S. E., Oman, L. D., Douglass, A. R., and Coy, L.: Modulation of Antarctic vortex composition by the quasi-biennial oscillation, *Geophys. Res. Lett.*, 42, 4216–4223, <https://doi.org/10.1002/2015GL063759>, 2015.
- 350 Turunen, E., Verronen, P. T., Seppälä, A., Rodger, C. J., Clilverd, M. A., Tamminen, J., Enell, C. F., and Ulich, T.: Impact of different energies of precipitating particles on NO_x generation in the middle and upper atmosphere during geomagnetic storms, *J. Atmos. Sol. Terr. Phys.*, 71, 1176–1189, <https://doi.org/10.1016/j.jastp.2008.07.005>, 2009.
- Wilks, D. S.: *Statistical methods in the atmospheric sciences*, vol. 100, Elsevier, 2011.